Local optical spectroscopy of semiconductor nanostructures in the linear regime

Local optical spectroscopy of semiconductor nanostructures in the linear regime

Oskar Mauritz, Guido Goldoni, and Elisa Molinari
Istituto Nazionale per la Fisica della Materia (INFM), and Dipartimento di Fisica, Università di Modena e Reggio Emilia, Via Campi 213A, I-41100 Modena, Italy

Fausto Rossi
Istituto Nazionale per la Fisica della Materia (INFM), and Dipartimento di Fisica, Politecnico di Torino, Corso Duca degli Abruzzi 24, I-10129 Torino, Italy

(Received 30 November 1999)

We present a theoretical approach to calculate the *local* absorption spectrum of excitons confined in a semiconductor nanostructure. Using the density-matrix formalism, we derive a microscopic expression for the nonlocal susceptibility, both in the linear and nonlinear regimes, which includes a three-dimensional description of electronic quantum states and their Coulomb interaction. The knowledge of the nonlocal susceptibility allows us to calculate a properly defined local absorbed power, which depends on the electromagnetic field distribution. We report on explicit calculations of the local linear response of excitons confined in single and coupled T-shaped quantum wires with realistic geometry and composition. We show that significant interference effects in the interacting electron-hole wave function induce new features in the space-resolved optical spectra, particularly in coupled nanostructures. When the spatial extension of the electromagnetic field is comparable to the exciton Bohr radius, Coulomb effects on the local spectra must be taken into account for a correct assignment of the observed features.

INTRODUCTION

The recent achievements in the field of semiconductor nanostructures have prompted a strong effort in developing local experimental probes in order to obtain spatial maps of the nanostructures and their quantum states. While conventional optical spectroscopy gives information on a large region containing thousands of nanostructures, confocal diffraction-limited microscopy has allowed the investigation of individual nanostructures.[1] To probe the spatial distribution of quantum states, the spatial resolution must be reduced much below the optical wavelength; this has been obtained by means of near-field scanning optical microscopy (NSOM).[2] In semiconductor quantum wires[3] and dots[4] the resolution of these experiments has been increasing in recent years.

From the theoretical point of view it was soon recognized that the interpretation of NSOM spectroscopic data requires us to take into account the effects of the fiber tip and dielectric discontinuities on the electromagnetic (EM) field generated in the sample. For example, the near-field distribution of the EM field[5] and its interaction with arrays of pointlike particles[6] have been studied in detail.

On the other hand, the interactions of a highly inhomogeneous EM field with the quantum states in the semiconductor nanostructures received much less attention.[7] A theoretical effort in this direction is important for different reasons. First, when the dipole approximation is abandoned and the nonlocal response of the medium is taken into account, local absorption itself is in principle ill defined (i.e., it is not independent of the EM-field distribution, as we will show); a general theoretical reformulation is therefore required. In addition, it may be expected that spatial interference of quantum states plays an important role when variations of the electromagnetic field occur on an ultrashort length scale, i.e., on the scale of the Bohr radius; hence, the necessity to describe the local absorption via a nonlocal susceptibility. The analogy with ultrafast time-resolved spectroscopies,[8] that have demonstrated the importance of phase coherence in the quantum-mechanical time evolution of photoexcited carriers,[9] suggests that similar effects may occur in the space domain.

To investigate the response of semiconductor nanostructures under these conditions, we have recently proposed[10] a theoretical approach based on a microscopic description of electronic quantum states and their Coulomb interaction. Our approach is intended to treat very high resolution probes, which might be capable of revealing Coulomb-induced coherence effects; therefore, we consider an inhomogeneous EM-field distribution with a spatial extension of the order of the Bohr radius of the material.[11] In this paper we describe in detail our theoretical approach and present absorption spectra calculated in the linear-response regime for a set of semiconductor quantum wires (QWR) with realistic geometry and composition, focusing on T-shaped structures as those obtained by the cleaved-edge overgrowth technique. We find that new features in the space-resolved optical spectra arise, particularly in coupled nanostructures, owing to interference effects in the interacting electron-hole wave function, and conclude that Coulomb effects on the local spectra must be taken into account for a correct assignment of the experimental features.

In Sec. I we derive the microscopic expression of the nonlocal susceptibility, including Coulomb interaction between electrons and holes, which is valid both in the linear and nonlinear regimes. In Sec. II we show how a proper

definition of local absorption can be introduced in the case of the spatially inhomogeneous EM field, which, however, depends on the shape of the EM-field distribution. In Sec. III we focus on the linear regime and we apply our scheme to single and coupled wire structures, studying, in particular, the effects of nonlocality and Coulomb interactions on local spectra.

I. THE NONLOCAL SUSCEPTIBILITY

In this section we derive a microscopic expression (i.e., based on microscopic electron and hole wave functions) of the nonlocal optical susceptibility $\boldsymbol{\chi}$; this will be obtained through a comparison between the macroscopic and the microscopic expressions for the optical polarization of the system. The knowledge of $\boldsymbol{\chi}$ allows us to calculate the absorbed power defined in Sec. II.

The macroscopic polarization $\mathbf{P}(\mathbf{r},t)$ induced by an electromagnetic field $\mathbf{E}(\mathbf{r},t)$ is in general given by

$$\mathbf{P}(\mathbf{r},t)=\int d\mathbf{r}'\int dt'\,\boldsymbol{\chi}(\mathbf{r},\mathbf{r}';t,t')\cdot\mathbf{E}(\mathbf{r}',t'), \tag{1}$$

where $\boldsymbol{\chi}(\mathbf{r},\mathbf{r}';t,t')$ is the nonlocal (both in space and time) susceptibility tensor. When the time dependence of $\boldsymbol{\chi}(\mathbf{r},\mathbf{r}';t,t')$ is through $t-t'$ only (stationary regime), the above equation can be transformed into a local equation in the frequency (ω) domain, i.e.,

$$\mathbf{P}(\mathbf{r},\omega)=\int \boldsymbol{\chi}(\mathbf{r},\mathbf{r}',\omega)\cdot\mathbf{E}(\mathbf{r}',\omega)\,d\mathbf{r}', \tag{2}$$

where $\mathbf{E}(\mathbf{r},\omega)$ and $\mathbf{P}(\mathbf{r},\omega)$ are the Fourier transforms of the time-dependent electric field and optical polarization in Eq. (1).

In the usual case of a homogeneous EM-field distribution the nonlocality of $\boldsymbol{\chi}$ is neglected, and $\boldsymbol{\chi}\propto\delta(\mathbf{r}-\mathbf{r}')$ in Eq. (2). In contrast, in order to describe the response of excitonic states to an EM field with a spatial extension which is comparable to the Bohr radius, the nonlocal character of $\boldsymbol{\chi}$ in Eq. (2) must be fully retained. Note also that, contrary to bulk states, excitonic states in a nanostructure do not have translational invariance; hence, $\boldsymbol{\chi}$ depends separately on the spatial coordinates $\mathbf{r}$, $\mathbf{r}'$ and not on the relative coordinate alone.

From a microscopic point of view the local (i.e., space-dependent) polarization can be written as

$$\mathbf{P}(\mathbf{r},t)=q\langle\hat{\boldsymbol{\Psi}}^{\dagger}(\mathbf{r},t)\mathbf{r}\hat{\boldsymbol{\Psi}}(\mathbf{r},t)\rangle, \tag{3}$$

where q is the electronic charge, $\langle\cdots\rangle$ denotes a proper ensemble average, and the field operator $\hat{\boldsymbol{\Psi}}(\mathbf{r},t)$ in the Heisenberg picture describes the microscopic time evolution of the carrier system.

Since in this paper we shall mainly focus on optical (i.e., electron-hole pairs) excitations, it is convenient to work within the so-called electron-hole picture. This corresponds to writing the field operator $\hat{\boldsymbol{\Psi}}(\mathbf{r},t)$ as a linear combination of electron and hole single-particle states,

$$\hat{\boldsymbol{\Psi}}(\mathbf{r},t)=\sum_e \hat{c}_e(t)\Psi_e(\mathbf{r})+\sum_h \hat{d}_h^{\dagger}(t)\Psi_h^*(\mathbf{r}), \tag{4}$$

where $\hat{c}_e$ and $\hat{d}_h$ denote destruction operators for an electron in state e and a hole in state h. Here e and h are appropriate sets of quantum numbers labeling the conduction and valence states involved in the optical transition, which are described by the single-particle wavefunctions $\Psi_{e/h}(\mathbf{r})$ and energy levels $\epsilon_{e/h}$.

By inserting the above electron-hole expansion into Eq. (3), and neglecting intraband contributions (absent for the case of optical excitations), the local polarization can be rewritten as

$$\mathbf{P}(\mathbf{r},t)=\sum_{eh}\,[p_{eh}(t)\mathbf{M}_{eh}^*(\mathbf{r})+\text{c.c.}], \tag{5}$$

where

$$\mathbf{M}_{eh}(\mathbf{r})=q\Psi_e^*(\mathbf{r})\mathbf{r}\Psi_h^*(\mathbf{r}) \tag{6}$$

is the local (i.e., space-dependent) dipole matrix element, and $p_{eh}(t)=\langle\hat{d}_h\hat{c}_e\rangle$ are nondiagonal (i.e., interband) elements of the single-particle density matrix, also referred to as interband polarizations.

Within the mean-field Hartree-Fock approximation, the time evolution of the above interband polarizations $p_{eh}(t)$ is described by the so-called semiconductor Bloch equations (SBE's),[12,13]

$$\frac{\partial}{\partial t}p_{eh}=\frac{1}{i\hbar}\sum_{e'h'}(\mathcal{E}_{ee'}\delta_{hh'}+\mathcal{E}_{hh'}\delta_{ee'})p_{e'h'}+\frac{1}{i\hbar}\mathcal{U}_{eh}(1-f_e-f_h)+\left.\frac{\partial p_{eh}}{\partial t}\right|_{coll}, \tag{7a}$$

$$\frac{\partial}{\partial t}f_e=\frac{1}{i\hbar}\sum_{h'}(\mathcal{U}_{eh'}p_{eh'}^*-\mathcal{U}_{eh'}^*p_{eh'})+\left.\frac{\partial f_e}{\partial t}\right|_{coll}, \tag{7b}$$

$$\frac{\partial}{\partial t}f_h=\frac{1}{i\hbar}\sum_{e'}(\mathcal{U}_{e'h}p_{e'h}^*-\mathcal{U}_{e'h}^*p_{e'h})+\left.\frac{\partial f_h}{\partial t}\right|_{coll}, \tag{7c}$$

where $f_e=\langle\hat{c}_e^{\dagger}\hat{c}_e\rangle$ and $f_h=\langle\hat{d}_h^{\dagger}\hat{d}_h\rangle$ denote electron and hole distribution functions, i.e., diagonal density-matrix elements. Here,

$$\mathcal{E}_{ee'}=\epsilon_e\delta_{ee'}-\sum_{e''}V_{ee''e'e''}f_{e''}, \tag{8}$$

$$\mathcal{E}_{hh'}=\epsilon_h\delta_{hh'}-\sum_{h''}V_{hh''h'h''}f_{h''}, \tag{9}$$

and

$$\mathcal{U}_{eh}=U_{eh}-\sum_{e'h'}V_{eh'he'}p_{e'h'} \tag{10}$$

are, respectively, the electron, hole and Rabi energies renormalized by the Coulomb interaction,[12–16] and

$$V_{ijkl}=\int d\mathbf{r}\int d\mathbf{r}'\Psi_i^*(\mathbf{r})\Psi_j^*(\mathbf{r}')V(\mathbf{r}-\mathbf{r}')\Psi_k(\mathbf{r}')\Psi_l(\mathbf{r}) \tag{11}$$

are the matrix elements of the three-dimensional Coulomb interaction $V(\mathbf{r}-\mathbf{r}')$ within the single-particle electron-hole representation. The last (collision) term in Eqs. (7) accounts for incoherent (i.e., scattering and diffusion) processes.[17]

In the usual case of a homogeneous (i.e., space-independent) optical excitation $\mathbf{E}^o$ the Rabi energy U_{eh} within the dipole approximation is given by

$$U_{eh}(t) = -\mathbf{M}^o_{eh}\cdot\mathbf{E}^o(t), \tag{12}$$

where

$$\mathbf{M}^o_{eh} = \int \mathbf{M}_{eh}(\mathbf{r})d\mathbf{r} \tag{13}$$

is the total dipole matrix element. In contrast, for the case of a local optical excitation $\mathbf{E}(\mathbf{r})$—the one considered in this paper—the electromagnetic field cannot be factorized as in Eq. (12) If, however, the space variation of the field is still negligible on the atomic scale, the Rabi energy for a local excitation is given by[18]

$$U_{eh}(t) = -\int \mathbf{M}_{eh}(\mathbf{r})\cdot\mathbf{E}(\mathbf{r},t)d\mathbf{r}. \tag{14}$$

Let us now focus on the stationary solutions of the SBE's (7). They can be easily found in the so-called quasiequilibrium regime, i.e., by assuming equilibrium distribution functions f_e, f_h which, therefore, do not depend on time; let us define the index $l=(e,h)$ and the matrices

$$T_{ll'} = \mathcal{E}_{ee'}\delta_{hh'} + \mathcal{E}_{hh'}\delta_{ee'}, \tag{15a}$$

$$W_{ll'} = V_{eh'he'}(1-f_e-f_h), \tag{15b}$$

$$S_{ll'} = T_{ll'} - W_{ll'}. \tag{15c}$$

Then, Eq. (7a) can be rewritten as

$$\frac{\partial p_l(t)}{\partial t} = \frac{1}{i\hbar}\sum_{l'} S_{ll'}p_{l'}(t) + \frac{1}{i\hbar}\overline{U}_l(t), \tag{16}$$

where $\overline{U}_l(t) = U_{eh}(t)(1-f_e-f_h)$.

Let us suppose that c^λ_l and Σ^λ are the eigenvectors and eigenvalues, respectively, of the matrix $S_{ll'}$; note that, in general, Σ^λ is complex. The eigenvector components c^λ_{eh} are the matrix elements of the unitary transformation connecting our original noninteracting basis $|eh\rangle$ with the excitonic basis $|\lambda\rangle$, $c^\lambda_{eh} = \langle eh|\lambda\rangle$. By applying this unitary transformation, we can rewrite Eq. (16) in the excitonic basis,

$$\frac{\partial p^\lambda(t)}{\partial t} = \frac{1}{i\hbar}\Sigma^\lambda p^\lambda(t) + \frac{1}{i\hbar}\overline{U}^\lambda(t), \tag{17}$$

where

$$p^\lambda(t) = \sum_l c^{\lambda *}_l p_l(t), \tag{18}$$

$$\overline{U}^\lambda(t) = \sum_l c^{\lambda *}_l \overline{U}_l(t). \tag{19}$$

If we Fourier transform Eq. (17) we find

$$p^\lambda(\omega) = -\frac{\overline{U}^\lambda(\omega)}{\Sigma^\lambda - \hbar\omega}, \tag{20}$$

$p^\lambda(\omega)$ and $\overline{U}^\lambda(\omega)$ being the Fourier transforms of $p^\lambda(t)$ and $\overline{U}^\lambda(t)$, respectively.

Let us consider again the local polarization field $\mathbf{P}(\mathbf{r},t)$ in Eq. (5), which in our excitonic picture λ, can be rewritten as

$$\begin{aligned}\mathbf{P}(\mathbf{r},t) &= \sum_\lambda [\mathbf{M}^{\lambda *}(\mathbf{r})p^\lambda(t) + \text{c.c.}] \\ &= \sum_\lambda \int_{-\infty}^{+\infty} [\mathbf{M}^{\lambda *}(\mathbf{r})p^\lambda(\omega) \\ &\quad + \mathbf{M}^\lambda(\mathbf{r})p^{\lambda *}(-\omega)]e^{-i\omega t}d\omega,\end{aligned} \tag{21}$$

with the definition $\mathbf{M}^\lambda(\mathbf{r}) = \Sigma_l c^{\lambda *}_l \mathbf{M}_l(\mathbf{r})$. By inserting the stationary solution (20), the dipole matrix element $\mathbf{M}^\lambda(\mathbf{r})$, and $\overline{U}^\lambda(\omega)$, we obtain

$$\begin{aligned}\mathbf{P}(\mathbf{r},\omega) = \int d\mathbf{r}' \sum_{\lambda,eh,e'h'} & c^\lambda_{eh}\mathbf{M}^*_{eh}(\mathbf{r}) \\ & \times c^{\lambda *}_{e'h'}\mathbf{M}_{e'h'}(\mathbf{r}')(1-f_{e'}-f_{h'}) \\ & \times \left[\frac{1}{\Sigma^\lambda - \hbar\omega} + \frac{1}{\Sigma^{\lambda *} + \hbar\omega}\right]\cdot\mathbf{E}(\mathbf{r}',\omega),\end{aligned} \tag{22}$$

$\mathbf{P}(\mathbf{r},\omega)$ being the Fourier transform of $\mathbf{P}(\mathbf{r},t)$. The above microscopic result has exactly the form of the macroscopic polarization in Eq. (1), thus providing the desired microscopic expression for the nonlocal optical susceptibility tensor $\boldsymbol{\chi}$. If we neglect the nonresonant term in Eq. (22) (the rotating-wave approximation), we obtain

$$\begin{aligned}&\boldsymbol{\chi}(\mathbf{r},\mathbf{r}',\omega) \\ &= \sum_{\lambda,eh,e'h'} \frac{c^\lambda_{eh}\mathbf{M}^*_{eh}(\mathbf{r}) \times c^{\lambda *}_{e'h'}\mathbf{M}_{e'h'}(\mathbf{r}')(1-f_{e'}-f_{h'})}{\Sigma^\lambda - \hbar\omega}.\end{aligned} \tag{23}$$

The above general expression describes the response of the system at the microscopic level, provided that the single-particle wave functions entering the local dipole matrix elements $\mathbf{M}_{eh}(\mathbf{r})$ are available. For the description of the response to a local probe with the extension comparable to the Bohr radius in a typical semiconductor, like GaAs, it is sufficient to describe the electron and heavy-hole states within the envelope function approximation, including fluctuations of the wave functions at the atomic scale only through bulk parameters. Assuming isotropic electron and heavy-hole energy dispersion, we write, as usual,[19] $\Psi_e(\mathbf{r}) = u_c(\mathbf{r})\psi_e(\mathbf{r})$ and $\Psi_h(\mathbf{r}) = u_v(\mathbf{r})\psi_h(\mathbf{r})$, where $\psi_{e/h}(\mathbf{r})$ are electron/hole envelope functions, and $u_{c/v}(\mathbf{r})$ are the atomic bulk wave functions at the conduction/valence edge. In this paper we consider only EM fields with a frequency corresponding to interband transition. Therefore, interpreting the space variables $\mathbf{r},\mathbf{r}'$ in Eq. (22) as coarse grained at the atomic scale, we can write

$$\mathbf{M}_{eh}(\mathbf{r}) = \mathbf{M}_b\psi^*_e(\mathbf{r})\psi^*_h(\mathbf{r}), \tag{24}$$

where $\mathbf{M}_b = \Omega_c^{-1}\int_{\Omega_c} u_c(\mathbf{r})\mathbf{r}u_v(\mathbf{r})d\mathbf{r}$ is the bulk dipole matrix element, with Ω_c the volume of the unit cell. Within such

approximation scheme, the susceptibility tensor $\boldsymbol{\chi}$ in Eq. (23) becomes diagonal, with identical elements given by

$$\chi(\mathbf{r},\mathbf{r}',\omega)=|M_b|^2\sum_{\lambda,eh,e'h'} c^{\lambda}_{eh}c^{\lambda *}_{e'h'} \times(1-f_{e'}-f_{h'})\frac{\psi_e(\mathbf{r})\psi_h(\mathbf{r})\psi^*_{e'}(\mathbf{r}')\psi^*_{h'}(\mathbf{r}')}{\Sigma^{\lambda}-\hbar\omega}. \tag{25}$$

II. LOCAL-ABSORPTION SPECTRUM

Given the susceptibility function in Eq. (25), the total absorbed power in a generic semiconductor structure can be evaluated according to

$$W(\omega)\propto\int d\mathbf{r}\int d\mathbf{r}'\,\mathrm{Im}[E(\mathbf{r},\omega)\chi(\mathbf{r},\mathbf{r}',\omega)E(\mathbf{r}',\omega)]. \tag{26}$$

In the usual definition of the absorption coefficient within the dipole approximation the nonlocality of χ is neglected: $\chi(\mathbf{r},\mathbf{r}')\propto\delta(\mathbf{r}-\mathbf{r}')$. When nonlocality is taken into account, it is no longer possible to define an absorption coefficient that locally relates the absorbed power density with the light intensity.

However, considering a light field with a given profile ξ centered around the beam position $\mathbf{R}$, $E(\mathbf{r},\omega)=E(\omega)\xi(\mathbf{r}-\mathbf{R})$, we may define a local absorption that is a function of the beam position, and relates the *total* absorbed power to the power of a *local* excitation (illumination mode):

$$\alpha_{\xi}(\mathbf{R},\omega)\propto\int \mathrm{Im}[\chi(\mathbf{r},\mathbf{r}',\omega)]\xi(\mathbf{r}-\mathbf{R})\xi(\mathbf{r}'-\mathbf{R})d\mathbf{r}\,d\mathbf{r}'. \tag{27}$$

This expression is in principle not limited to low-photoexcitation intensities; via f_e, f_h appearing in Eq. (25) it provides a general description of linear as well as nonlinear local response, i.e., from excitonic absorption to the gain regime. On the other hand, in the linear-response regime $1-f_e-f_h\simeq 1$ and the quantity $\Psi^{\lambda}(r_e,r_h)=\Sigma_{eh}c^{\lambda}_{eh}\psi_e(r_e)\psi_h(r_h)$ can be identified with the exciton wave function; in this case the explicit form of the local-absorption coefficient (27) can be written as

$$\alpha_{\xi}(\mathbf{R},\omega)=\mathrm{Im}\left[\sum_{\lambda}\frac{\alpha^{\lambda}_{\xi}(\mathbf{R},\omega)}{\Sigma^{\lambda}-\hbar\omega}\right], \tag{28}$$

where

$$\alpha^{\lambda}_{\xi}(\mathbf{R},\omega)\propto\left|\int\Psi^{\lambda}(\mathbf{r},\mathbf{r})\xi(\mathbf{r}-\mathbf{R})\,d\mathbf{r}\right|^2. \tag{29}$$

The effects of spatial coherence of quantum states are easily understood in the linear regime on the basis of Eq. (29). For a spatially homogeneous EM field, the absorption spectrum probes the average of Ψ^{λ} over the whole space (global spectrum). In the opposite limit of an infinitely narrow probe beam, $\alpha^{\lambda}_{\xi}(\mathbf{R},\omega)$ maps $|\Psi^{\lambda}|^2$; the local absorption is nonzero at any point where the exciton wave function gives a finite contribution. It is, therefore, clear that ''forbidden'' excitonic transitions, not present in the global spectrum, may appear in the local one. In the intermediate regime of a narrow but finite probe, it is possible that a cancellation of the contributions from Ψ^{λ} at different points in space takes place, leading to a nontrivial localization of the absorption. The result will then be quite sensitive to the extension of the light beam.

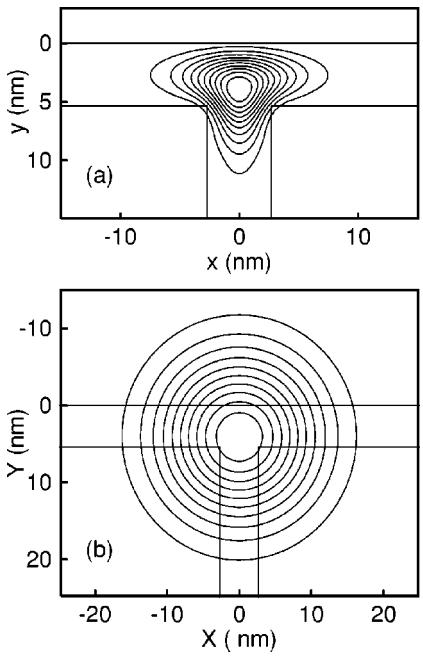

FIG. 1. (a) Effective wave function [Eq. (A3)] for the ground-state exciton of a single T-shaped GaAs/AlAs quantum wire obtained at the intersection between two quantum wells of width 5.4 nm. The electron-hole interaction is taken into account (12 subbands included in the calculation of the polarization). Only the real part is plotted; the imaginary part is negligible. (b) Contribution of the same ground-state exciton to the local absorption, $\alpha_{\xi}(X,Y,\omega^{\lambda})$ [see Eq. (A1)], calculated for an EM field ξ with Gaussian distribution and $\sigma=10$ nm. The T-wire confinement profile is shown as a reference in both panels.

III. NUMERICAL RESULTS

The theoretical formulation of Secs. I and II is valid for semiconductors of arbitrary dimensionality. To illustrate the effects of nonlocality and Coulomb interaction on the local absorption spectrum, we now consider quasi-one-dimensional (1D) nanostructures (quantum wires), subject to a local EM excitation propagating parallel to the free axis of the structure z. For simplicity, we describe the narrow light beam by a Gaussian EM field profile, $\xi(\mathbf{r})=\exp[-(x^2+y^2)/2\sigma^2]$.[20] The explicit expressions for quasi-1D systems are derived in the Appendix.

As a prototype system, we have chosen to investigate systems composed of GaAs/AlAs T-shaped QWR's, which rank among the best available samples from the point of view of optical properties, and allow for a strong quantum confinement.[21,22]

In Fig. 1(a) we show the ground-state effective wave function [Eq. (A3)] for a single QWR, including the electron-hole interaction; the exciton is strongly localized at the intersection of the parent QW's, the localization being

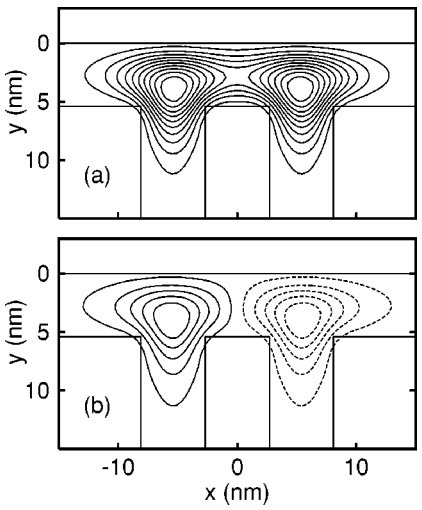

FIG. 2. Effective wave function [Eq. (A3)] for (a) the ground state and (b) the first excited state in structure composed of two symmetric T-shaped quantum wires, each obtained at the intersection of two GaAs/AlAs wells. The real part is plotted in (a) while the imaginary part is negligible; the opposite applies to (b). Both the parent QW's and the barrier between the vertical stems are 5.4 nm wide. Coulomb interaction is taken into account (two subbands included in the calculation of the polarization). The confinement profile is shown in both panels for reference.

dominated by that of the hole state which has a heavier effective mass.[21] When the effect of a locally inhomogeneous EM field with a Gaussian shape ($\sigma=10$ nm) is simulated [Fig. 1(b)], we find that the signal exibits a maximum at the location of the exitonic wave function, but the details of the shape of the wave function are lost as, for this particular sample, they take place on a scale shorter than σ.

The above situation for a single QWR can be contrasted with the situation for two coupled QWR's. In the latter case the exitonic states of the two QWR's are coupled by Coulomb interaction if their mutual distance is $\sim a_B$; therefore, in this case the nonlocal character of the Coulomb interaction can be exposed by a local probe with $\sigma \sim a_B$. To exemplify this, we show in Fig. 2 the effective wave function of (a) the ground and (b) the first excited excitonic states for two coupled, symmetric QWR's, including electron-hole Coulomb interaction. It should be noted that (1) the two excitonic states confined in the two QWR's are strongly coupled by effect of the Coulomb interaction and (2) the effective wave function is not positive definite but is even or odd for the ground and first excited state, respectively; as a consequence, in a homogenous EM field only the ground state appears in the spectrum, while the first excited state is prohibited by a selection rule arising from the cancellation between positive and negative regions [see Eq. (29)]. This selection rule is relaxed in a local optical spectroscopy experiment, if variations of the EM field takes place on a scale comparable to the modulations of the effective wave function. In fact, when the center of mass of the beam does not coincide with a symmetry point of the structure, the symmetry of the whole system is broken; consequently, cancellations do not take place exactly; moreover, they are a function of the position and extension of the beam.

It should be stressed that the spatial dependence of the absorption in the coupled QWR structure is dominated by Coulomb interaction, thus making very high resolution local optical spectroscopy a very powerful tool. To demonstrate this aspect, we have simulated a local optical spectroscopy experiment by calculating the local absorption spectra while sweeping the tip of the probe across a double-QWR structure; the influence of interwire Coulomb interaction is demonstrated in Fig. 3, where full calculations including electron-hole interaction (center panels) are compared with calculations where the correlation is switched off (left panels). For this example we have chosen a set of asymmetric structures composed of two sligthly different QWR's, with various distances between the stems of the wires. In the uncorrelated spectra we can only distinguish two peaks arising from single-particle transitions localized in either wires; the two peaks shift in energy as a function of the interwire distance, decreasing from top to bottom, as a result of the increasing overlap between the single-particle states localized in the two QWR's, and are accompained by a high-energy tail which is due to the single-particle joint density of states. Note that there is no sign of spatially indirect transitions connecting an electron and a hole localized in different wires.

The situation is very different when Coulomb correlation is taken into account. First, we note that for the larger wire separation (top row) (i) the two main peaks, arising from a direct transitions located in either wires, are red-shifted by the exciton binding energy, and (ii) the high-energy continua are suppressed, as expected from previous studies of total absorption in quasi-1D structures.[14] When the interwire distance is decreased, new peaks appear in the spectra whose energy, intensity, and location is strongly dependent upon the coupling between the two wires, which increases from top to bottom in Fig. 3. These peaks result from interference between positive and negative regions of the effective wave functions, whose square modulus is shown in the right column for comparison. Figure 4 compares the local spectra obtained with a tip position located in the center of the right and left wire with the total absorption for the same set of coupled QWR's as in Fig. 3.[23]

CONCLUSIONS

In summary, we have developed a general formulation of the theory of local optical absorption in semiconductor nanostructures, taking into account quantum confinement of electron and hole states and the electron-hole Coulomb interaction. We have proved that absorption is strongly influenced by the spatial interference in the exciton wave functions, which depends on the profile of the light beam. When the extension of the beam becomes comparable with the exciton Bohr radius, local spectra are expected to display different features with respect to integrated spectra, resulting from the breaking of selection rules. Calculations performed for a set of coupled quantum wires show that the interpretation of near-field experiments will require a quantitative treatment of these effects as their spatial resolution increases.

ACKNOWLEDGMENTS

We thank C. Simserides for a careful reading of this manuscript. This work was supported in part by INFM

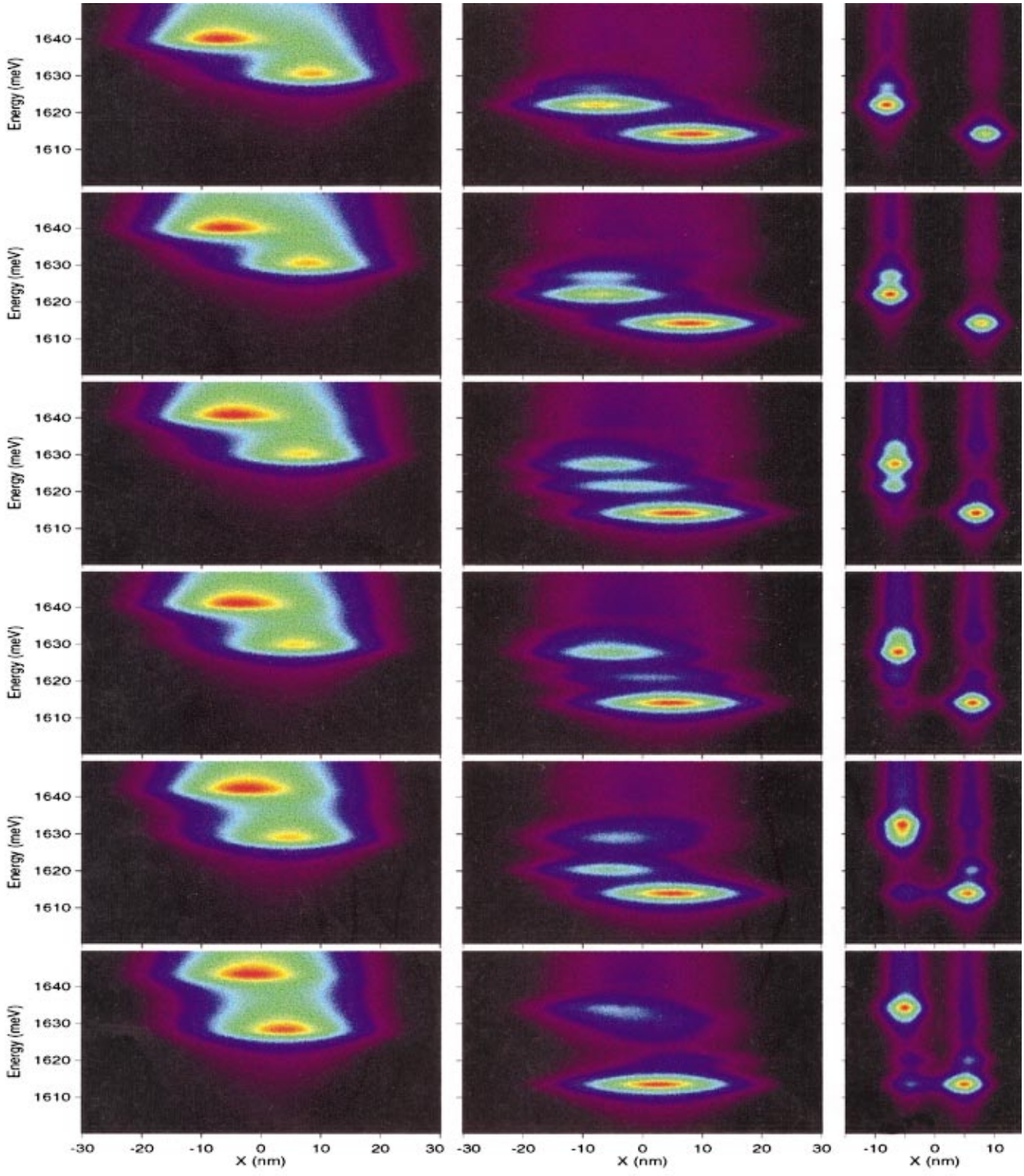

FIG. 3. (Color) Calculated local absorption $\alpha(X,Y,\hbar\omega)$ as a function of photon energy and beam position for a set of asymmetric T-shaped quantum wires whose coupling is decreasing from the top to the bottom row. Left column: the spectra are calculated in the single-particle approximation. Central column: full calculation including electron-hole Coulomb interaction. Right column: square modulus of the effective wave function. Two subbands were included in the calculations. The three panels in each row refer to the same structure, obtained at the intersection between an horizontal QW (5.4 nm wide), and two vertical QW's (the left QW is 5.4 nm wide and the right QW is 6.0 nm wide). The vertical QW's are separated by a distance d equal to (from top to bottom) 10.8, 9.6, 8.0, 6.8, 5.4, and 4.4 nm. The tip position X is swept across the structure along a line positioned in the middle of the horizontal QW; the EM field distribution is Gaussian, with $\sigma=10$ nm, and a broadening $\Gamma=2$ meV is included in the calculation.

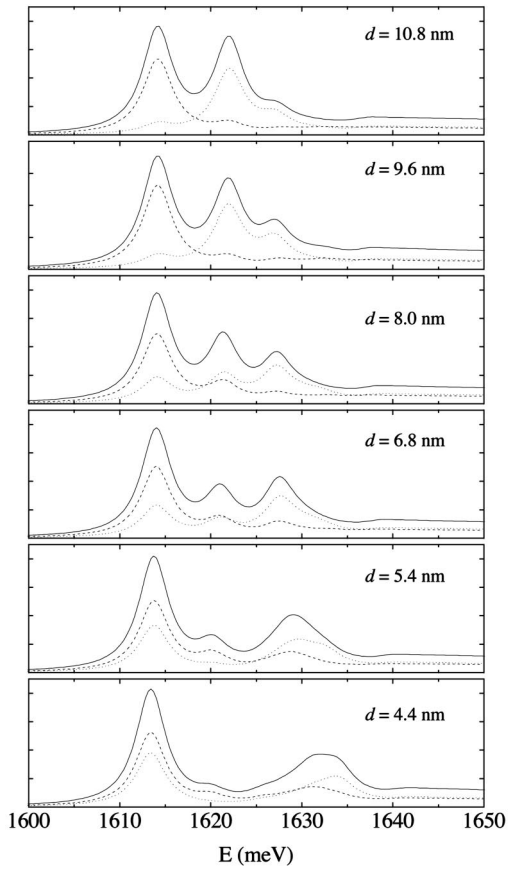

FIG. 4. Global (solid line) and local absorption spectra (including electron-hole correlation), calculated with the beam centered on the right wire (dashed line) and on the left wire (dotted line) for the same set of nanostructures as in Fig. 3 (same order from top to bottom). Here $\sigma=10$ nm and an artificial inhomogeneous broadening ($\Gamma=2$ meV) is included.

through PRA ''PROCRY,'' and by the EC under the TMR Network ''Ultrafast'' and the IT-project ''SQID.''

APPENDIX: CALCULATION OF THE LOCAL ABSORPTION IN THE LINEAR REGIME FOR QUASI-1D SYSTEMS

For a QWR the single-particle electron and hole envelope functions, appearing in Eq. (25), can be written as $\psi_e(\mathbf{r})=\phi^e_{\nu_e}(x,y)e^{ik^e_z z}$ and $\psi_h(\mathbf{r})=\phi^h_{\nu_h}(x,y)e^{ik^h_z z}$, respectively, where $\nu_{e/h}$ and $k^{e/h}_z$ are subband indices and wave vectors along the free axis. The envelope functions $\phi^{e/h}_\nu(x,y)$ are solutions of a Schrödinger equation with effective masses and band parameters appropriate for electron and heavy-holes in the two-dimensional (2D) confinement potential of the QWR.

In the linear regime the local absorption can be written as [Eq. 29]

$$\alpha_\xi(X,Y,\omega)\propto\sum_\lambda\left|\int\Phi^\lambda(x,y)\xi(x-X,y-Y)dx\,dy\right|^2\times h(\omega-\omega^\lambda), \tag{A1}$$

where ω^λ is the resonance frequency, $h(\omega)$ describes the line broadening, and

$$\Phi^\lambda(x,y)\equiv\int\Psi^\lambda(\mathbf{r},\mathbf{r})\,dz. \tag{A2}$$

We shall refer to $\Phi^\lambda(x,y)$ as the *effective exciton wave function*; according to Eq. (A1), when convoluted with the spatial distribution of the EM field, $\xi(x-X,y-Y)$, $\Phi^\lambda(x,y)$ yields the contribution of the λth excitonic state to the local absorption $\alpha_\xi(X,Y,\omega)$.

Taking advantage of the translational invariance along z we have

$$\Phi^\lambda(x,y)=\sum_{\nu_e\nu_h}P^\lambda_{\nu_e\nu_h}\phi^e_{\nu_e}(x,y)\phi^h_{\nu_h}(x,y), \tag{A3}$$

where we have defined $P^\lambda_{\nu\nu'}=\Sigma_{k_z}c^\lambda_{\nu k_z\nu'-k_z}$. Note that only Fourier components of the polarization with $k^e_z=-k^h_z$ contribute to the absorption.

In our calculations we use a plane-wave basis set to represent the (x,y) dependence of the single-particle wave functions,

$$\phi^{e/h}_\nu(x,y)=\frac{1}{\sqrt{L_xL_y}}\sum_{n_xn_y}c^{e/h,\nu}_{n_xn_y}e^{i(k_xx+k_yy)}, \tag{A4}$$

where $k_\alpha=2\pi n_\alpha/L_\alpha$ and $\alpha=x,y$. From Eqs. (A3) and (A4) we get

$$\Phi^\lambda(x,y)=\sum_{\nu_e\nu_h}P^\lambda_{\nu_e\nu_h}\sum_{n^e_xn^e_y}c^{e,\nu_e}_{n^e_xn^e_y}e^{i(k^e_xx+k^e_yy)}\sum_{n^h_xn^h_y}c^{h,\nu_h}_{n^h_xn^h_y}e^{i(k^h_xx+k^h_yy)}. \tag{A5}$$

Therefore, we can write

$$\Phi^\lambda(x,y)=\sum_{n_xn_y}C^\lambda_{n_xn_y}e^{i(k_xx+k_yy)}, \tag{A6}$$

where the Fourier coefficients $C^\lambda_{n_xn_y}$ are given by

$$C^\lambda_{n_xn_y}=\sum_{\nu_e\nu_h}P^\lambda_{\nu_e\nu_h}\left(\sum_{n^e_xn^e_yn^h_xn^h_y}{}'\;c^{e,\nu_e}_{n^e_xn^e_y}c^{h,\nu_h}_{n^h_xn^h_y}\right), \tag{A7}$$

and the primed summation is subjected to the conditions $n^e_x+n^h_x=n_x, n^e_y+n^h_y=n_y$.

Finally, if ξ can be factorized as $\xi(x,y)=\xi_x(x)\xi_y(y)$, as is the case of a Gaussian, then the integral in Eq. (A1) is given by

$$\int\Phi^\lambda(x,y)\xi(x-X,y-Y)\,dx\,dy=\sum_{n_xn_y}C^\lambda_{n_xn_y}\hat\xi_x(k_x)\hat\xi_y(k_y)e^{i(k_xX+k_yY)}, \tag{A8}$$

where

$$\hat\xi_\alpha(k_\alpha)=\frac{1}{2\pi}\int\xi_\alpha(\alpha)e^{-ik_\alpha\alpha}\,d\alpha. \tag{A9}$$

[1] See, e.g., A. Zrenner, L.V. Butov, and M. Hagn, Phys. Rev. Lett. **72**, 3382 (1994); D. Gammon, E.S. Snow, and D. Park, *ibid.* **76**, 3005 (1996); J. Hasen, L.N. Pfeiffer, and B.S. Dennis, Nature (London) **390**, 54 (1997).

[2] E. Betzig and R.J. Chichester, Science **262**, 5138 (1993); H.F. Hess, E. Betzig, and T.D. Harris, *ibid.* **264**, 1740 (1994).

[3] R.D. Grober, T.D. Harris, and J.K. Trautman, Appl. Phys. Lett. **64**, 1421 (1994); T.D. Harris, D. Gershoni, and N. Chand, *ibid.* **68**, 988 (1996); Ch. Lienau, A. Richter, and K.H. Ploog, Phys. Rev. B **58**, 2045 (1998); V. Emiliani, Ch. Lienau, and R. Cingolani, *ibid.* **60**, 13 335 (1999).

[4] Y. Toda, M. Kourogi, and M. Ohtsu, Appl. Phys. Lett. **69**, 827 (1996); A. Chavez-Pirson, J. Temmyo, H. Kamada, H. Gotoh, and H. Ando, *ibid.* **72**, 3494 (1998); H. Zhou, A. Midha, G. Mills, L. Donaldson, and J.M.R. Weaver, *ibid.* **75**, 1824 (1999).

[5] R. Chang, P.-K. Wei, W.S. Fann, M. Hayashi, and S.H. Lin, J. Appl. Phys. **81**, 3369 (1997).

[6] B. Hanewinkel, A. Knorr, and S.W. Koch, Phys. Rev. B **55**, 13 715 (1997).

[7] G.W. Bryant, Appl. Phys. Lett. **72**, 768 (1998).

[8] J. Shah, *Ultrafast Spectroscopy of Semiconductors and Semiconductor Nanostructures* (Springer, Berlin, 1996).

[9] A.P. Heberle, J.J. Baumberg, and K. Kohler, Phys. Rev. Lett. **75**, 2598 (1995).

[10] O. Mauritz, G. Goldoni, F. Rossi, and E. Molinari, Phys. Rev. Lett. **82**, 847 (1999).

[11] This is at difference with, e.g., Ref. 6 and A. Knorr, F. Steininger, and S.W. Koch, Phys. Status Solidi B **206**, 139 (1998), where a broader EM field is considered and, accordingly, excitonic states are treated as pointlike dipoles.

[12] H. Haug and S.W. Koch, *Quantum Theory of the Optical and Electronic Properties of Semiconductors*, 3rd ed. (World Scientific, Singapore, 1994).

[13] T. Kuhn, in *Theory of Transport Properties of Semiconductor Nanostructures*, edited by E. Schöll (Chapman & Hall, London, 1998), p. 173.

[14] F. Rossi and E. Molinari, Phys. Rev. Lett. **76**, 3642 (1996); Phys. Rev. B **53**, 16 462 (1996).

[15] F. Rossi, Semicond. Sci. Technol. **13**, 147 (1998).

[16] In Eq. (4) of Ref. 10 only the diagonal renormalized Rabi energies were included. This corresponds to neglect intraband polarizations which are expected to be very small. Obviously, off-diagonal Rabi energies are exactly zero in the linear regime.

[17] For a discussion of these effects at different temperatures in quantum wires see A. Richter, G. Behme, M. Süptitz, Ch. Lienau, and T. Elsaesser, Phys. Rev. Lett. **79**, 2145 (1997). In our calculations we treat the collision term within the relaxation time approximation.

[18] A. Stahl and I. Balslev, *Electrodynamics of the Semiconductor Band Edge*, Springer Tracts in Modern Physics, Vol. 110 (Springer, Berlin, 1987).

[19] In the present calculations valence-band mixing is neglected [see G. Goldoni, F. Rossi, E. Molinari, and A. Fasolino, Phys. Rev. B **55**, 7110 (1997)].

[20] The actual profile of the EM field generated by a NSOM tip is more complex, and a research topic in itself. However, our simple choice for ξ is sufficient to highlight the effects of nonlocality. Any field distribution can be included in our treatment through Eq. (29), while Eq. (25) is independent of the external field.

[21] F. Rossi, G. Goldoni, and E. Molinari, Phys. Rev. Lett. **78**, 3527 (1997), and references therein.

[22] We use homogeneous and isotropic effective masses $m^e = 0.067 m_0$ and $m^h = 0.34 m_0$; the GaAs/AlAs band offsets are $V^e = 1.033$ eV and $V^h = 0.558$ eV.

[23] For clarity, in the present calculations we have neglected higher-energy states from the wider QW. We have checked that these do not affect the local spectra in Fig. 4, but would only contribute to the high-energy part of the global spectrum in the same figure.